# Preparation, Structural Characterization, and Properties of Poly(methyl methacrylate)/Montmorillonite Nanocomposites by Bulk Polymerization

**Xiongwei Qu, Tonghua Guan, Guodong Liu, Qingyan She, Liucheng Zhang**

*Institute of Polymer Science and Technology, School of Chemical Technology, Hebei University of Technology, Tianjin, 300130, People's Republic of China*

Received 18 November 2003; accepted 15 November 2004
DOI 10.1002/app.21749
Published online in Wiley InterScience (www.interscience.wiley.com).

**ABSTRACT:** Poly(methyl methacrylate) (PMMA)/montmorillonite (MMT) nanocomposites were synthesized by a simple technique of a monomer casting method, bulk polymerization. The products were purified by hot acetone extraction and characterized by Fourier transform infrared spectroscopy, X-ray diffraction (XRD), transmission electron microscopy (TEM), differential scanning calorimetry (DSC), thermogravimetric analysis (TGA), examination of their mechanical properties, and light transmittance testing. Although XRD data did not show any apparent order of the MMT layers in the nanocomposites, TEM revealed parallel MMT layers with interlamellar spacings of an average of 9.8 nm and the presence of remnant multiplets of nonexfoliated layers. Therefore, PMMA chains were intercalated in the galleries of MMT. DSC and TGA traces also corroborated the confinement of the polymer in the inorganic layer by exhibiting the increase of glass-transition temperatures and mass loss temperatures in the thermogram. Both the thermal stability and the mechanical properties of the products appeared to be substantially enhanced, although the light transmittances were not lost. Also, the materials had excellent mechanical properties. Measurement of the tensile properties of the PMMA/MMT nanocomposites indicated that the tensile modulus increased up to 1013 MPa with the addition of 0.6 wt % MMT, which was about 39% higher than that of the corresponding PMMA; the tensile strength and Charpy notched impact strength increased to 88 MPa and 12.9 kJ/m$^2$, respectively. As shown by the aforementioned results, PMMA/MMT nanocomposites may offer new technology and business opportunities.  J Appl Polym Sci 97: 348–357, 2005

**Key words:** mechanical properties; nanocomposites; thermogravimetric analysis (TGA)

## INTRODUCTION

In recent years, polymer-layered silicate nanocomposites have received great attention and have been highlighted. This is mainly because of the possibility that these kinds of materials could have unique properties with a much higher modulus and heat-distortion temperature,[1–5] unusual thermal stability,[6–9] and excellent barrier properties of gas and water[10–14] compared with pristine polymers. One of the most promising approaches to the synthesis of these materials consists of the dispersal of an inorganic clay mineral in an organic polymer on a nanometer scale. This concept was first introduced by researchers from Toyota, who discovered the possibility of building a nanocomposite from polyamide 6 and organic clay.[15] The new materials showed dramatic improvements in thermal and mechanical properties. Numerous other researchers later used this concept for nanocomposites based on epoxies,[5,16,17] unsaturated polyester,[18] polystyrene,[4,19] polyimide,[10,11] poly(ethylene oxide),[20,21] and so on. These materials were produced either by melt intercalation of thermoplastics or by *in situ* polymerization.[1,2,13,17,19,20,22]

The structural characteristics of montmorillonite (MMT) are two fused silica tetrahedral sheets sandwiching an edge-shared octahedral sheet. Isomorphous substitutions of $Si^{4+}$ for $Al^{3+}$ in the tetrahedral lattice and of $Al^{3+}$ for $Mg^{2+}$ in the octahedral sheet cause an excess of negative charges within the MMT layers. These negative charges are counterbalanced by cations such as $Ca^{2+}$ and $Na^{+}$ situated between the MMT layers. However, the presence of polar hydroxyl groups in the MMT impedes nonpolar species from fully entering the galleries and exfoliating the MMT.

Poly(methyl methacrylate) (PMMA) is a transparent (>90% transmission), hard, stiff material with excellent ultraviolet stability, low water absorption, and high abrasion resistance. It is very stable in high electrical fields and releases little smoke on combustion. The material has poor fatigue resistance with a continuous temperature of around 50°C. It is rather brittle

*Correspondence to:* X. Qu (xwqu@263.net).
Contract grant sponsor: Natural Science Foundation of Hebei Province; contract grant number: 201006.
Contract grant sponsor: China Scholarship Council.

(notch sensitive) and exhibits stress cracking in most organic solvents. PMMA has outstanding outdoor weathering properties. It is mainly used for static applications, such as glazing in the form of double-skinned, ribbed sheets for greenhouses. It is also used for lighting covers (diffusers). External applications include shop signs, transparent covers (e.g., sight glass), and certain grades of resin concrete.

Because of their outstanding properties, PMMA products are widely used in microelectronic and aerospace industries.[23] Recently, PMMA/MMT hybrids have been studied.[12,24,25] Studies on PMMA/MMT nanocomposites have mainly been directed toward the elucidation of the effect of the inclusion of MMT on the barrier properties and the characterization of the nanometer structures.[12] The plasticizer permeability of the PMMA/MMT nanocomposites in poly(vinyl chloride) blends were lowered compared with the pristine poly(vinyl chloride). However, there has been little study on the effect of MMT on the mechanical properties of PMMA. This prompted us to explore PMMA-intercalated MMT nanocomposites by bulk polymerization. It was worth it to study the effect of the inclusion of the MMT nanolayer on the mechanical properties, especially the tensile properties and thermal properties for the PMMA/MMT nanocomposites.

In this investigation, a bulk polymerization in which the MMT was dispersed in the methyl methacrylate (MMA) monomer phase and polymerized with an organic initiator, was carried out in the presence of $Na^+$-exchanged MMT. This article discusses the results obtained from the structural study and material characterization of nanocomposites prepared by aforementioned bulk polymerization.

## EXPERIMENTAL

### Materials

Sodium ion MMT was supplied by Huate Bentonite Co. (Linan, China) with a cation-exchange capacity of 115 mequiv/100 g. We freed the MMA monomer (Tianjin Chemical Co., Tianjin, China) of inhibitor by washing it with a 1–2% sodium hydroxide solution, followed by repeated washing with distilled water. The monomer was then dried over $CaCl_2$ and distilled under reduced pressure before use. All other reagents, analytical pure grade, were used as supplied.

The MMT was purified first by the removal the heavy mineral impurities by sedimentation in water and then by dialysis against distilled water to remove soluble salts. The purified MMTs were dried under reduced pressure at 60°C for 24 h. The MMTs were ground in a mortar and pestle and micronized to give a particle size of approximately 2 $\mu$.

### Bulk polymerization

MMA monomers (100 g) containing 0.2 wt % benzoyl peroxide (BPO) initiator and a measured amount of MMT were added to a conical flask. The compositions of MMA/MMT were 100/0, 99.8/0.2, 99.6/0.4, 99.4/0.6, 99.2/0.8, and 99/1.0 w/w. The blends were stirred for 2 h to achieve complete dispersion of MMT into the MMA monomer. After being sonicated for 30 min with a KQ-250 sonicator (Jiangshu Kunshan Ultrasonic Instrument Co., Kunshan, China) at room temperature with a water bath at 90°C, the flask was equipped with a magnetic stirrer charged with nitrogen. The increased surface area of fine MMT particles was formed by sonication in the MMA monomer before the bulk polymerization. When the viscosity of the partially polymerized syrup was increased to 2000 mPa, the mixture was outgassed in a vacuum oven for a short period of time and poured into a glass plate mold. The clamped assembly was put in an oven, first at a temperature of 40°C to continue the polymerization for 24 h and then at a temperature of 100°C for 1.5 h to complete the polymerization process.

### Characterization and measurement

Free PMMA was separated from the PMMA/MMT adduct by extraction of the blend with boiling acetone for 2 days by means of Soxhlet extraction, precipitated into methanol, and finally dried in a vacuum oven at 60°C for 48 h for molecular weight measurement. The molecular weight was determined by the viscometric measurements to obtain the intrinsic viscosity[11] and the viscosity-average molecular weight ($M_\eta$) according to the Mark–Houwink equation, where $k$ is equal to $5.5 \times 10^{-3}$ and $\alpha = 0.73$, when acetone was the flow phase at 25°C.[26] An Ulman viscosity meter (Tianjin, China) with a concentration of 0.1 g/100 mL was used:

$$[\eta] = kM_\eta^{\alpha}$$

The Fourier transform infrared (FTIR) spectra for PMMA and PMMA/MMT nanocomposites with different MMT contents were recorded on a Bruker spectrophotometer (Vector-22) (Ettlingen, Germany) in the range 1850–1300 $cm^{-1}$. Care was taken to press all of the KBr pellets at the same conditions to minimize any effects of pressure on the peak frequencies for the powder samples. We recorded X-ray diffraction (XRD) patterns by monitoring the diffraction angle ($2\theta$) from 1 to 20° on a DMAX-RC X-ray diffractometer (Rigaku Co., Tokyo, Japan). The unit was equipped with a Ni-filtered Cu K$\alpha$ radiation source operated at 50 kV and 180 mA. The scanning speed was 1°/min. The morphological aspects of the hybrid materials were examined with transmission electron microscopy (TEM) to determine the internal micrograph. A Hita-

chi H-800 transmission electron microscope (Tokyo, Japan) with an acceleration voltage of 100 kV was used. Ultrathin sections were analyzed without staining. The thermal properties of the composites were measured by differential scanning calorimetry (DSC; Dupont 2000, DSC-2910) and thermogravimetric analysis (TGA; Dupont 2000 SDT-2960) (New Castle, DE). We took DSC measurements by heating each sample up to 200°C at a heating rate of 10°C/min under a nitrogen atmosphere. To assure identical thermal histories, all samples were heated to 200°C, cooled, and heated again to determine the glass-transition temperature ($T_g$) during the second heating cycle. We took TGA measurements by heating each sample to 800°C at a heating rate of 20°C/min under a nitrogen atmosphere. The initial decomposition temperatures (5 and 10% mass loss) were given out by a computer program. The tensile properties were measured on an Instron (model 1122) tensile machine (Buckinghamshire, UK) according to ASTM D 638 with a crosshead speed of 5 mm/min at room temperature. The Charpy notched impact tests on the specimens were carried out with a pendulum-type impact tester (CXJ-40, Chengde Testing Instruments, Inc., Chengde, China) at room temperature. At least five runs were made so we could report the average. The light transmittance test was done with a HY-10 light transmittance tester (Shanghai, China) according to GB241 0-88.

## RESULTS AND DISCUSSION

### Structural characterization

The PMMA/MMT composites obtained by bulk polymerization were exposed to boiling acetone for 2 days to remove free PMMA macromolecules. The polymerization produced nonextractable PMMA/MMT adducts up to an extent of 30%. According to McEwan,[27] the forces to which the adsorbed molecules are subjected are dipolar attractions and van der Waals forces. In heating, BPO and BPO/MMT will form free radicals, some of which will remain attached to the MMT surface.[28,29] In the presence of a monomer, free radical will yield homopolymer, which may become attached or anchored to the MMT surface. Most of the growth takes place either in the intercalated MMA or with the MMA that is solvated loosely to bound chains. The inserted polymer, resulting from the polymerization of monomer inserted in the layers between the lamellae, is then accompanied by a certain amount of polymer formed outside the lamellae (external polymer). The former can be extracted with polar solvents, and the latter is impossible to extract. The interaction between PMMA and the silicate laver was studied by FTIR (Fig. 1). A part of the PMMA/MMT composite (0.6 wt %) was extracted with hot acetone for 2 days to remove the nonbonded PMMA. The unextractable PMMA, which could be regarded as the bonded PMMA, was verified by FTIR spectra, as shown in Figure 1. As shown in Figure 1(b), the FTIR spectrum of the residual hybrid product from the Soxhlet extraction gave a distinct absorption at 1735 $cm^{-1}$ (C═O stretching) due to the characteristic frequencies of PMMA. This result might be ascribed to the PMMA as being intercalated and to hydrogen-bond formation between the oxygen of the polymer molecules and the hydroxyl of the MMT lattice.[30] As shown in Table I, the products holding unextractable organic materials, which could be regarded as the bonded PMMA, revealed different quantities of bound polymer. The trend appeared to be that the contents of the unextractable polymer were inversely proportional to the amount of MMT added.

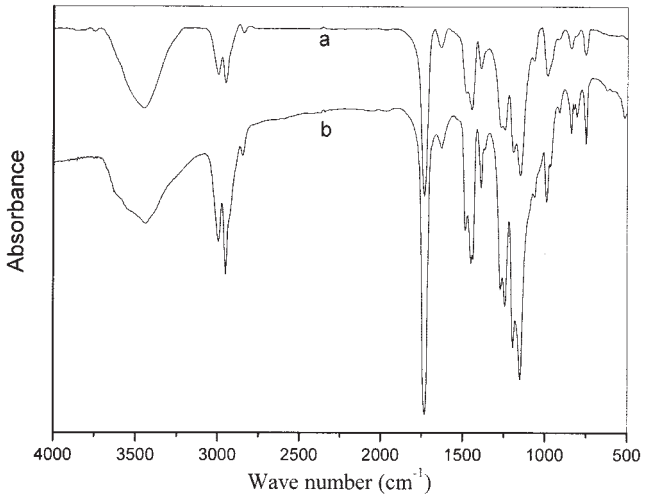


**Figure 1** FTIR spectra of (a) pure PMMA and (b) the residual product extracted from the PMMA/MMT composite (0.6 wt %).

**TABLE I**
**$M_\eta$ values of PMMA Obtained from the Composite Extracts**

| MMT content in the PMMA/MMT composites | | | |
|---|---|---|---|
| A | B | $[\eta]$ | $M_\eta \times 10^{-5}$ |
| 0 | 0 | 47.3 | 2.46 |
| 0.2 | 11.0 | 49.8 | 2.63 |
| 0.4 | 17.6 | 52.2 | 2.81 |
| 0.6 | 26.8 | 53.9 | 2.94 |
| 0.8 | 38.5 | 55.9 | 3.09 |
| 1.0 | 39.7 | 58.5 | 3.28 |

The products in column A were not purified by extraction. The products in column B were purified by boiling acetone extraction for 2 days. $[\eta]$ is the intrinsic viscosity.

The $M_\eta$ values of external PMMA recovered from the composite extracts are summarized in Table I. A trend that was obvious, as shown in Table I, was that the molecular weights of the polymers obtained from

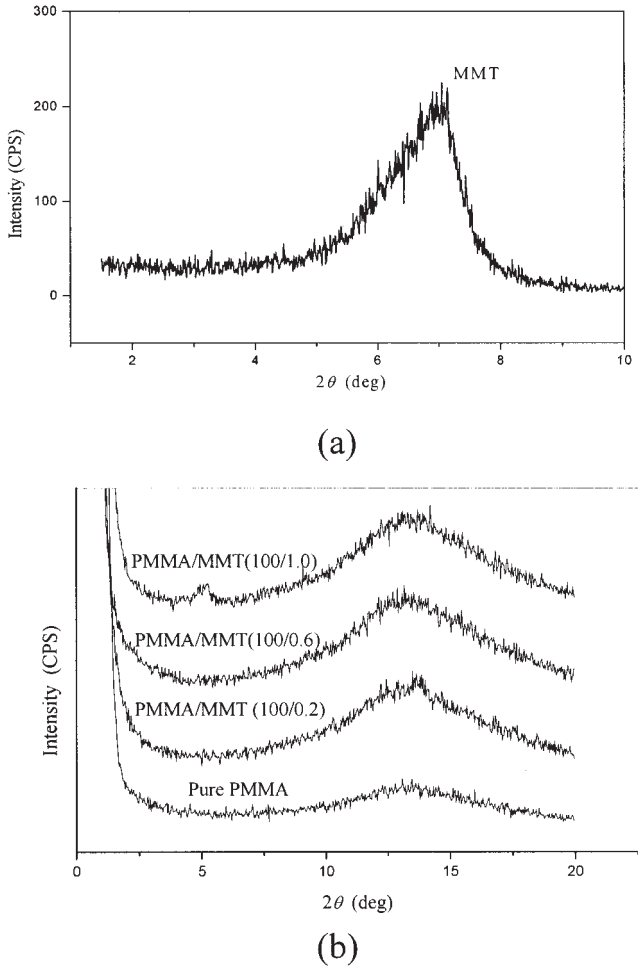


**Figure 2** XRD patterns of (a) MMT and (b) pure PMMA and PMMA/MMT nanocomposites with different MMT contents.


**Figure 3** TEM microgram of a PMMA/MMT composite (0.6 wt %).

the composite were not only higher than the molecular weight of pure PMMA but also proportional to the amount of MMT added. This suggests that the presence of MMT significantly increased the average molecular weight of the polymer. All the molecular weight data were of direct relevance to indicate that the intercalation of the molecular weight of the polymer, although not straight, may have been equivalent to those values listed in Table I.

Further evidence for the intercalation was obtained from the XRD patterns of the PMMA/MMT composites. As shown by the powder patterns in Figure 2, the peak observed in MMT at $2\theta = 7.1°$ ($d = 1.20$ nm) [Fig. 2(a)], corresponding to the basal spacing of MMT, disappeared in the hybrids [Fig. 2(b)], suggesting disorder and a loss of structural regularity in the MMT layers. Meanwhile, a peak situated around $2\theta = 12.5°$ was observed for all of the MMT contents. This peak corresponded to the amorphous phase of PMMA, characterizing its arrangement of macromolecules.[31] The presence of this peak was important because it demonstrated that the XRD analysis was sufficiently sensitive to detect the presence of the MMT in the nanocomposites.

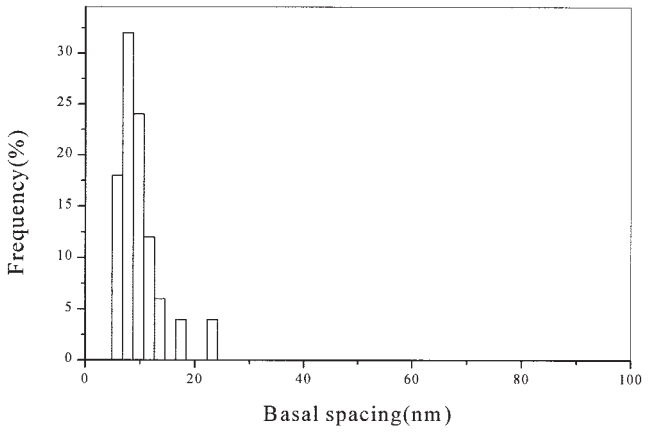


**Figure 4** Frequency diagram of basal spacing obtained by TEM for a PMMA/MMT composite (0.6 wt %).

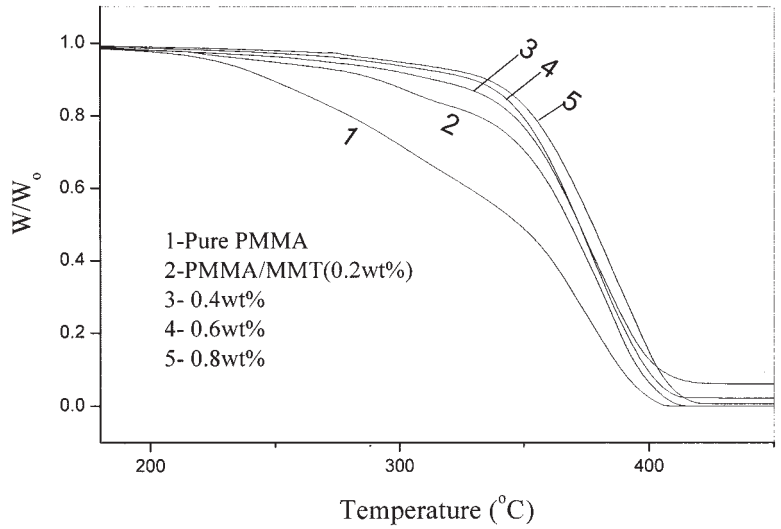


**Figure 5** TGA thermogram of pure PMMA and nanocomposites with different MMT contents. $W/W_0$ is the ratio of the residual weight to the initial weight of the sample.

Although XRD allowed for precise measurements of the silicate layer spacing, little could be said about the real spatial position of the layers or any change in the structure of the composites. The featureless patterns could not suggest the presence of intercalated or delaminated hybrids. So, TEM analysis was added to examine the microstructure of the hybrids. TEM provided information in real space, in a local area on the spatial distribution of the silicate layers, of the changes of the structure in the hybrids. Figure 3 is a TEM photograph of the PMMA/MMT composite containing 0.6 wt % of MMT. Because the silicate layers were composed of heavier elements (Al, Si, and O) than the interlayer and surrounding matrix (C, H, and N), they appeared darker in the bright-field images. The overall picture showed that the MMT layers did not occupy the full volume and that layer regions of the pure PMMA matrix were visible. At this scale, considerable inhomogeneity, rather than a monolithic structure, was apparent. A closer observation of the micrograph at high magnification revealed that each dark line often corresponded to several MMT layers. The presence of those multiplets was also observed by Noh et al. in styrene–acrylonitrile copolymer/MMT nanocomposites.[32] This interesting detail in the nanocomposites demonstrated that the MMA monomer did not diffuse into all of the MMT galleries during the polymerization process. As a consequence, all of the layers were not separated individually on polymerization. The average distance between the stacks of layers evaluated from the overall picture was around 9.8 nm. The frequency diagram of basal spacing obtained by TEM is shown in Figure 4. This was in good agreement with the XRD results, where no basal (001) re-

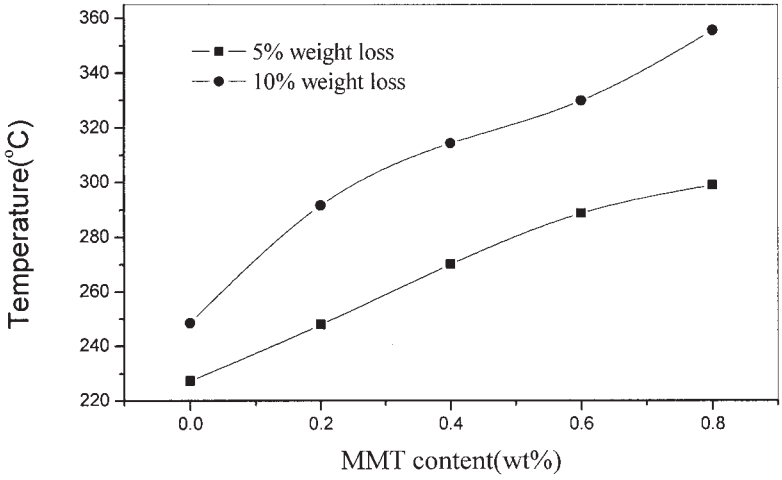


**Figure 6** Effect of MMT content on the 5 and 10% decomposition of the PMMA/MMT nanocomposites.

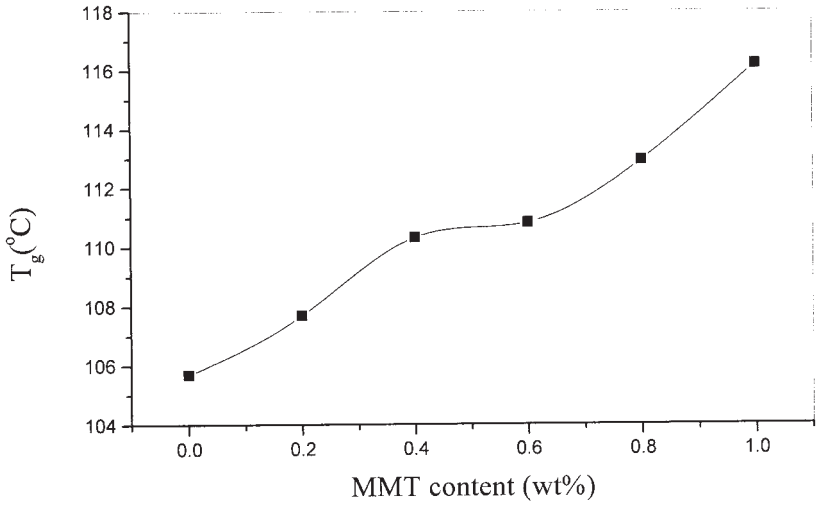


**Figure 7** Effect of the MMT content on the $T_g$ from DSC traces of the PMMA/MMT nanocomposites.

flection was observed. TEM micrographs showed that the PMMA/MMT nanocomposite had a very similar structural nature to the intercalated composite. Particularly interesting was that the sample was mostly homogeneous with no phase separation between the silicate layers and the PMMA matrix.

Polar organic molecules can form monomolecular, bimolecular, or trimolecular layers between the lamella. Blumstein suggested that the MMA/MMT complex were two monomer layers laying flat between each pair of silicate lamella.[29] Therefore, TEM measurement of the interlamellar spacings after polymerization showed that the inserted polymer molecule was laying flat on the surface of the lamellae, covering the enormous surface of the lamellar planes.

These results indicate that the nanocomposite was successfully prepared by the simple technique of bulk polymerization. Therefore, the PMMA/MMT composite could also lead to the production of an effective nanocomposite without with any kind of coupling agents or modifications of the monomer. Also, the nonextractable products revealed about 30 wt % polymer content on average, which was more strong evidence of intercalation.

## Thermal properties

The TGA results recorded for the PMMA/MMT nanocomposites monitored the effect of the MMT on the thermal properties. Figure 5 shows a TGA thermogram of the weight loss as a function of the temperature for pure PMMA and PMMA/MMT nanocomposites containing various amounts of MMT. The thermal decomposition temperature of the PMMA/MMT nanocomposites increased with increasing MMT content in the range studied. The temperature at 5 wt % loss of PMMA/MMT increased by 20 and 72°C on the basis of PMMA for MMT contents of 0.2 and 0.8 wt %, respectively. The thermal stability of the nanocomposites increased with MMT loading. The temperatures at 5 and 10% weight loss are shown in Figure 6, which indicates that the thermal stability of the PMMA was enhanced by the incorporation of only a small number of MMT layers. An inserted polymer is always less degraded thermally, even when the external polymer is subjected to oxidative degradation, because oxygen cannot penetrate between the lamellae. The external polymer, on the other hand, was occluded in the microvoids existing between the crystallites of the MMT. This allowed for rapid diffusion of the monomer away from the reaction centers and favored the degradation of the polymer. It appeared that the stability of the inserted polymer was due to not only its particular structure but also to steric factors restricting the ther-

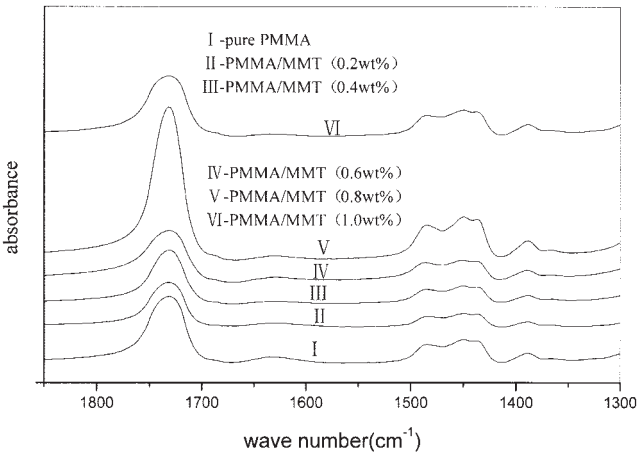


**Figure 8** Selected regions of FTIR absorbance spectra with various methyl and carbonyl modes of the PMMA/MMT nanocomposites.

**TABLE II**
**Peak Area Ratios of $\delta_{CH3}$ to $\nu_{C=O}$ in different PMMA/MMT Systems**

| | PMMA/MMT | | | | | |
|---|---|---|---|---|---|---|
| | 100/0 | 99.8/0.2 | 99.6/0.4 | 99.4/0.6 | 99.2/0.8 | 99/1.0 |
| $S_1/S_2$ | 0.0458 | 0.0428 | 0.0412 | 0.0408 | 0.0397 | 0.0369 |

mal motion of the segments sandwiched between the two lamellae.[33] The unzipping of the chains began when the temperature was high enough to bring about this motion. Thus, the PMMA macromolecules synthesized through the polymerization of the nanolayer inserted between the lamellae of the MMT seemed to be shielded from external influences, and their thermal stability seemed to become noticeably enhanced.

$T_g$ was used to describe the chain segment's motion. From the DSC curves, the $T_g$ of the pure PMMA was about 105.69°C.[34] Figure 7 shows the effect of the MMT content on the $T_g$ from the DSC curves. It was confirmed that the $T_g$'s of the PMMA/MMT nanocomposites increased with increasing MMT content: the $T_g$ values were 107.69, 110.31, 110.81, 112.92, and 116.17°C at MMT contents of 0.2, 0.4, 0.6, 0.8, and 1.0 wt %, respectively. Because the glass-transition process is related to molecular motion, $T_g$ is considered to be affected by molecular packing, chain rigidity, and linearity.[35] The increase in the $T_g$'s of the nanocomposites in comparison with the original PMMA were attributed to the maximization of the adhesion between the polymer and layered silicate surfaces. Because of the nanometer size that restricted segmental motion near the organic inorganic interface, it was a typical effect for the inclusion of MMT in a polymer system.[36]

In addition to the perfect thermal insulation effect of MMT and the strong interaction between MMT layers and macromolecules, there was another possible mechanism that accounted for the enhanced thermal stability. We studied the termination mechanism of PMMA in nanocomposites with different contents of MMT by means of FTIR spectroscopy.

MMA bulk polymerization follows classical free-radical polymerization chemistry and consists of four basic steps, initiation, propagation, chain transfer, and chain termination.

The chain-termination process may have played an important role in the determination of the polymer thermal stability, which resulted in the consumption of radicals and ended the polymerization process. There are basically two chain-termination processes (in addition to chain transfer, which terminates a growing radical chain, but also generates a new one). Termination by combination results in a head-to-head reaction of growing chains [(1) in the structure]. Here, the carbon–carbon bond, formed by a combination of two tertiary-substituted free radicals, is weak and relatively thermally unstable. Termination by disproportionation is the result of hydrogen transfer from one growing radical to another to yield an unsaturated polymer end [(2) in the structure] and a saturated end [(3) in the structure]:

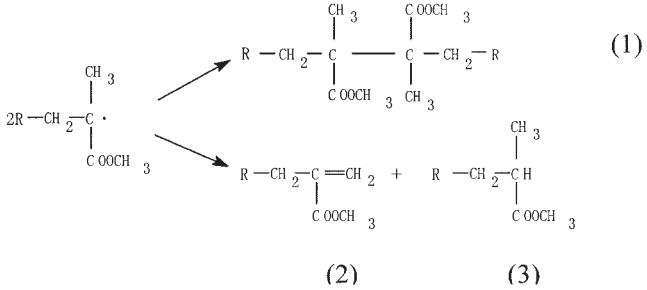


The thermogravimetric decomposition temperature of these groups as measured on model compounds yielded approximate degradation temperatures. If the termination occurs by combination, the degradation temperature of the formed chains (1) will be around 190°C.[41] However, if the termination is by disproportionation, then the degradation temperatures of the formed polymer chains containing the unsaturated (2) and saturated (3) end-groups should be around 255°C and >300°C, respectively.[41] The decomposition temperatures terminated by disproportionation were higher than those of combination. Thus, the type and amount of these chain-termination groups directly influenced the thermal stability of the polymer.

FTIR spectrometry offers excellent analytical features for the detection and determination of inorganic and organic compounds.[37–40] As the FTIR absorbance

**TABLE III**
**Mechanical Properties of Different Nanocomposites and Pure PMMA**

| | MMT content (wt %) | | | | | |
|---|---|---|---|---|---|---|
| | 0 | 0.2 | 0.4 | 0.6 | 0.8 | 1.0 |
| Tensile strength (MPa) | 68 | 77 | 81 | 88 | 85 | 80 |
| Tensile modulus (MPa) | 730 | 810 | 913 | 1013 | 1051 | 1103 |
| Tensile elongation (%) | 9.31 | 9.50 | 8.87 | 8.69 | 8.10 | 7.30 |
| Charpy impact strength (kJ/cm$^2$) | 8.42 | 9.70 | 10.45 | 12.86 | 12.06 | 11.55 |

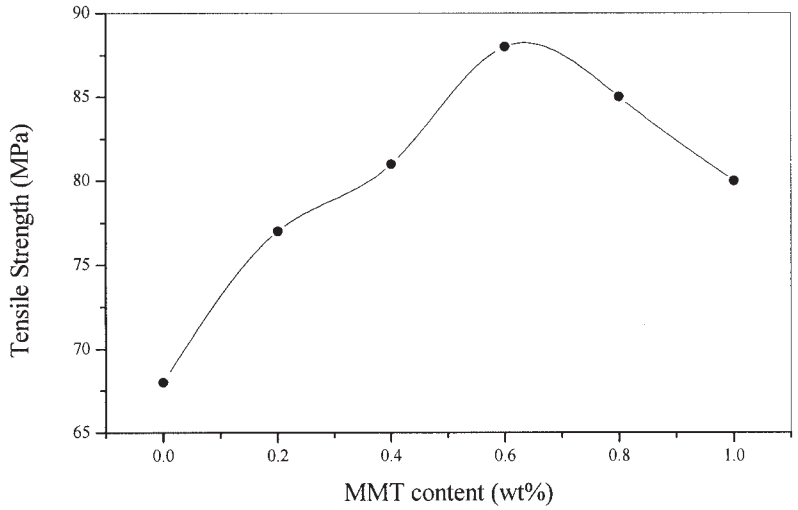


**Figure 9** Effect of MMT content on the tensile strength of the PMMA/MMT nanocomposites (sonication time = 0.5 h).

(Fig. 8) of the carbonyl group $\nu_{C=O}$ at 1740 $cm^{-1}$ was not affected by the termination mode, we used the peak area of the carbonyl group $\nu_{C=O}$ as a reference band. Although the number of the methyl group $\delta_{CH3}$ depended on the termination mechanism, the peak area of $\delta_{CH3}$ increased with increasing coupling termination of end radicals. So, we used the ratios of the integrated peak area of $\delta_{CH3}$ ($S_1$) to that of $\nu_{C=O}$ ($S_2$) in the FTIR spectroscopy of the ranges 1415–1371 and 1847–1664 $cm^{-1}$, respectively, to characterize content of combination to disproportionation to express the change in the PMMA macromolecules. The results are listed in Table II. The values of $S_1/S_2$ decreased with the addition of MMT. This means that the ratios of termination by disproportionation increased with the addition of MMT. Therefore, the thermal stability of PMMA increased with the addition of MMT.

## Mechanical and light properties

The tensile properties of the PMMA nanocomposites were examined and are listed in Table III. The effects of the MMT content on the mechanical properties of the PMMA/MMT nanocomposites are summarized in Figures 9–11. Clearly, the MMT nanolayers, even when aggregated in the form of intercalated layers, strengthened, stiffened, and toughened the matrix. The tensile modulus of the composite apparently increased in proportion to the amount of MMT. With the incorporation of 0.6% MMT, the tensile modulus increased to about 1.01 GPa, which was about 39% higher than that of the original PMMA. The addition of 1% MMT further increased the modulus to 1.10 GPa, which was about 51% higher than the pristine PMMA. This enhancement of modulus was reason-

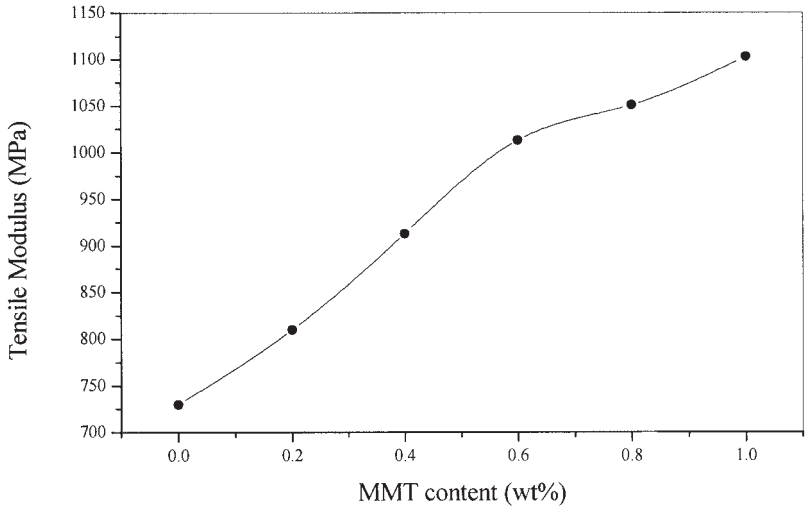


**Figure 10** Effect of MMT content on the tensile modulus of the PMMA/MMT nanocomposites (sonication time = 0.5 h).

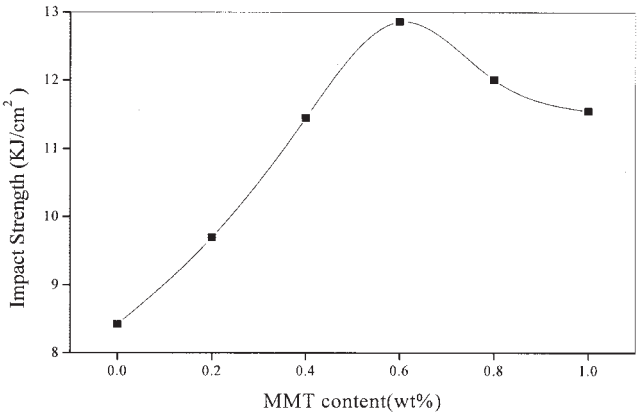


**Figure 11** Effect of MMT content on the Charpy impact strength of the PMMA/MMT nanocomposites (sonication time = 0.5 h).

ably attributed to the high resistance exerted by the MMT against the plastic deformation, together with the effect of the stretching resistance of the oriented backbone bonds of the polymer chain in the gallery. The tensile strength approached the highest point at about 0.6 wt % and decreased with further increases in MMT content because of the lower elongation at break. The notched impact strength increased rapidly with MMT content to 0.6 wt %, about 12.06 kJ/m$^2$, an increase of 52% over the pristine PMMA, but changed little for MMT contents over 0.8 wt %.

It is very unusual to improve modulus and at the same time significantly improve the strength, and the modulus is directly attributable to the reinforcement provided by the dispersed silicate nanolayers.

On exposure to mechanical stresses, anisotropic particles can orient to form nanovoids, which are very effective stress concentrators. This process can dissipate energy at the crack tip throughout the sample volume. Moreover, on straining, the individual layers of the larger superstructure undergo shearing, similar to a process typical for metals. Therefore, many intercalated structures with fairly large superstructures give a much better impact performance with respect to intercalated nanocomposites. These results indicate that PMMA/MMT nanocomposites have potential for industry.

To increase the dispersion of MMT in the MMA monomer, sonication technology was used because of the high surface energy of MMT. This was probably the consequence of an increased surface area of fine MMT particles that were formed by sonication in the MMA monomer before the bulk polymerization. This was an indication that the sonication disentangled the aggregated particles and, hence, increased the surface area of the MMT. The mechanical property data of the PMMA/MMT (99.4/0.6) composites at different sonication times are summarized in Table IV. The influence of sonication time on the mechanical properties was obvious when the sonication time was between 0.5 and 1.5 h. The effect leveled off above 1.5 h. The maximum data of the tensile strength, tensile modulus, and Charpy notched impact strength increased by 32.2, 60.3, and 68.6%, respectively, compared with the corresponding PMMA.

**TABLE V**
**Light Transmittance Value of the PMMA/MMT Nanocomposites**

| MMT content (wt %) | 0 | 0.2 | 0.4 | 0.6 | 0.8 |
|---|---|---|---|---|---|
| Transmittance (%) | 92.1 | 94.0 | 94.1 | 94.0 | 94.3 |

Another significant property of the PMMA/MMT nanocomposites was their high optical transparency. The transparency of the nanocomposites came from the dispersion of the MMT nanolayer into the PMMA sheet. As shown in Table V, the MMT particles at high contents could completely disperse into nanolayer, and even if some remained as aggregates, the transparencies of the PMMA/MMT nanocomposites did not lessen. Because the nanocomposites may have had phase domains smaller than the wavelength of light, the materials were transparent.

## CONCLUSIONS

The most striking results obtained from the previous experiments were the demonstrations of direct intercalation to the smectic type of MMT by a simple bulk polymerization and the enhanced properties of the intercalated products. The PMMA/MMT nanocomposites synthesized by bulk polymerization had the following characteristics:

**TABLE IV**
**Influence of Sonication Time on the Mechanical Properties of the PMMA/MMT (0.6 wt %) Nanocomposites**

| | Sonication time (h) | | | | | | |
|---|---|---|---|---|---|---|---|
| | 0.5 | 1.0 | 1.5 | 2.0 | 3.0 | 4.0 | 5.0 |
| Tensile strength (MPa) | 88 | 91 | 90 | 88 | 90 | 89 | 87 |
| Tensile modulus (MPa) | 1013 | 1170 | 1170 | 1163 | 1170 | 1180 | 1158 |
| Charpy impact strength (kJ/m$^2$) | 12.86 | 13.68 | 14.20 | 14.08 | 14.15 | 14.31 | 14.19 |

1. The tensile modulus was enhanced by the inclusion of the MMT layers into the PMMA matrix, accompanied by an increase in the notched impact strength. The increase in the mechanical properties was almost solely due to the reinforcement effect of the dispersed MMT layers. At 0.6% MMT loading, the PMMA/MMT nanocomposites showed the best balance in properties with regard to the modulus, impact strength, $T_g$, and thermal stability due to the intercalated dispersion of the MMT in the PMMA matrix.
2. $T_g$'s of the nanocomposites were higher than the $T_g$'s of the pristine PMMA, and the PMMA/MMT nanocomposites had higher thermal stabilities compared to the pristine PMMA. The enhanced thermal stabilities of the composites were also corroborated by the TGA experiments.
3. The PMMA/MMT nanocomposites comprised an acetone-extractable PMMA and an acetone-insoluble PMMA/MMT intercalation with a particle size on the order of 9.8 nm as revealed by TEM analysis. The structural analysis of the composites confirmed that the PMMA chains were confined between the interlayer of MMT in the form of a stretched planar type of conformation.

## References


1. Kojima, Y.; Usuki, A.; Kawasumi, M.; Okada, A.; Kurauchi, T.; Kamigaito, O. J Polym Sci Part A: Polym Chem 1993, 31, 1755.
2. Liu, L.; Qi, Z.; Zhu, X. J Appl Polym Sci 1999, 71, 1133.
3. Ke, Y.; Long, C.; Qi, Z. J Appl Polym Sci 1999, 71, 1139.
4. Harotaka, N.; Okamoto, H.; Kawasumi, M.; Usuki, A. J Appl Polym Sci 1999, 74, 3359.
5. Messersmith, P. B.; Giannelis, E. P. Chem Mater 1994, 6, 1719.
6. Wang, S.; Long, C.; Wang, X.; Li, Q.; Qi, Z. J Appl Polym Sci 1998, 69, 1557.
7. Lee, D. C.; Jang, L. W. J Appl Polym Sci 1996, 61, 1117.
8. Biwas, M.; Ray, S. S. J Appl Polym Sci 2000, 77, 2948.
9. Wang, C.; Pinnavaia, T. J. Chem Mater 1998, 10, 3769.
10. Zhu, Z. K.; Yang, Y.; Yin, J.; Wang, X.; Ke, Y.; Qi, Z. J Appl Polym Sci 1999, 73, 2063.
11. Yano, K.; Usuki, A. J Appl Polym Sci 1993, 31, 2493.
12. Chen, G.; Yao, K.; Zhao, J. J Appl Polym Sci 1999, 73, 425.
13. Messersmith Philips, B.; Giannelis, E. P. J Polym Sci Part A: Polym Chem 1995, 33, 1047.
14. Burnside, S. D.; Giannelis, E. P. Chem Mater 1995, 7, 1597.
15. Okada, A.; Kawasumi, M.; Kurauchi, T.; Kamigaito, O. Polym Prepr 1987, 28, 447.
16. Giannelis, E. P.; Messersmith Philips, B. U. S. Pat. W096/08526 (1996).
17. Kormmann, X.; Lindberg, H.; Berglund, L. A. Polymer 2001, 42, 1303.
18. Kommann, X.; Berglund, L. A.; Sterte, J.; Giannelis, E. P. Polym Eng Sci 1998, 38, 1351.
19. Chen, G.; Ma, Y.; Qi, Z. J Appl Polym Sci 2000, 77, 2201.
20. Vaia, R. A.; Sauer, B. B.; Tse, O. K.; Giannelis, E. P. J Polym Sci Part B: Polym Phys 1997, 35, 59.
21. Aranda, P.; Ruiz-Hitzky, E. Chem Mater 1992, 4, 1395.
22. Noh, M. H.; Lee, D. C. J Appl Polym Sci 1999, 74, 2811.
23. Cholod, M. S.; Parker, H. Y. In Polymeric Materials Encyclopodia; CRC: Boca Raton, FL, 1996; p 6385.
24. Okamoto, M.; Morita, S.; Kim, Y. H.; Kotaka, T.; Tateyama, H. Polymer 2001, 42, 1201.
25. Zeng, C.; Lee, L. J. Macromolecules 2001, 34, 4098.
26. He, M.; Chen, W.; Dong, X. Polymer Physics; Fudan University Press: Shanghai, 1993.
27. McEwan, D. M. C. Trans Faraday Soc 1948, 44, 349.
28. Dekking, H. G. G. J Appl Polym Sci 1967, 11, 23.
29. Blumstein, A. J Polym Sci Part A: Gen Pap 1965, 3, 2653.
30. Bhattacharya, J.; Chakravarti, S. K.; Talapatra, S.; Saha, S. K.; Guhaniyogi, S. C. J Polym Sci Part A: Polym Chem 1989, 27, 3977.
31. Zhou, G. X-Ray Diffraction for Polymer; China University of Science and Technology Press: Hefei, China, 1989.
32. Noh, M. H.; Lee, W. J.; Lee, D. C. J Appl Polym Sci 1999, 74, 179.
33. Blumstein, A. J Polym Sci Part A: Gen Pap 1965, 3, 2665.
34. Guan, T. MSc. Thesis, Hebei University of Technology, 2002.
35. Li, F.; Ge, J.; Honigfort, P.; Fang, S.; Chen, J.; Harris, F.; Cheng, S. Polymer 1999, 40, 4987.
36. Agag, A.; Takeichi, T. Polymer 2000, 41, 7083.
37. Eliades, G.; Vougiouklakis, G.; Palaghias, G. Dent Mater 2001, 17, 277.
38. Novaki, L. P.; Correa, N. M.; Silber, J. J.; EI Seoud, O. A. Langmuir 2000, 16, 5573.
39. Kurtz, S. M.; Muratoglu, O. K. Biomaterials 2001, 22, 1731.
40. Quintas, G.; Armenta, S.; Morales-Noe, A.; et al. Anal Chim Acta 2003, 480, 11.
41. Cacioli, P.; Moad, G.; Rizzardo, E.; Derelis, A. K.; Solomon, D. H. Polym Bull 1984, 11, 325.